Research Square

Preprints are preliminary reports that have not undergone peer review.
They should not be considered conclusive, used to inform clinical practice,
or referenced by the media as validated information.

Optimal superdense coding through noisy channels by escorting qubits

Javid Ahmad Malik
National Institute of Technology Srinagar
Muzaffar Qadir Lone
lone.muzaffar@uok.edu.in

University of Kashmir
Prince A Ganai
National Institute of Technology Srinagar

Article

Keywords:

Posted Date: February 26th, 2026

DOI: https://doi.org/10.21203/rs.3.rs-8764753/v1

License: This work is licensed under a Creative Commons Attribution 4.0 International License. Read Full License

Additional Declarations: No competing interests reported.

Optimal superdense coding through noisy channels by escorting qubits

Javid Ahmad Malik[1], Muzaffar Qadir Lone[2],* and Prince A Ganai[1]

We introduce an escort-qubit–assisted protocol that restores and stabilizes superdense coding capacity in the presence of amplitude damping channel (ADC) noise. The protocol is analyzed under three fundamental noisy configurations: amplitude damping acting on Alice's subsystem, on Bob's subsystem, and on both subsystems covering all practically relevant scenarios. In the absence of protection, we show that ADC effects cause a monotonic degradation of the superdense coding capacity, driving it below the classical limit in the strong decoherence regime and completely erasing the quantum advantage. Our escort-qubit protocol overcomes this limitation by coherently tracking the channel-induced Kraus trajectories during entanglement distribution. Post-selection of the no-flip trajectory, projects the shared state onto a maximally entangled resource state, thereby recovering the optimal superdense coding capacity of two classical bits, independent of the noise strength and noisy configuration. Importantly, when all ADC trajectories are taken into account, the resulting average capacity although inherently suboptimal remains strictly above both the classical limit and the unprotected capacity across the entire decoherence range. These results establish the escort-qubit protocol as a powerful, scalable, and experimentally viable approach for preserving quantum advantage and enhancing information throughput in noisy quantum communication networks.

1. INTRODUCTION

Superdense coding represents a remarkable and elegant demonstration of how quantum entanglement enables non-local information processing. It holds both foundational importance in quantum information theory and practical relevance for quantum communication technologies. In the seminal proposal [1], it was shown that a sender can transmit two bits of classical information using only one qubit, provided that the communicating parties share initially a maximally entangled state. This effectively doubles the information capacity compared to what is possible through classical means alone. Building on this concept, superdense coding has been generalized to higher-dimensional multipartite quantum systems [2–6], as well as to atomic and cavity QED systems [7–11], and even to continuous-variable frameworks [12–15]. Experimentally, the protocol has been successfully realized using different physical implementations, including linear optical setups and nuclear magnetic resonance systems [16–21].

The capacity of superdense coding is defined as the maximum amount of classical information that can be reliably transmitted to the receiver, given a specific initial shared state. In the ideal, noise-free scenario, it is generally accepted that the maximum capacity of superdense coding is given by $C = \log d$, where d denotes the dimension of the sender's subsystem [22–27]. However, in practical physical systems, this theoretical limit is rarely achievable. For instance, in linear optical implementations, the capacity is restricted due to the impossibility of performing a complete Bell-state measurement [28]. In other physical platforms, the inevitable influence of environmental noise further diminishes the effective channel capacity. Consequently, in recent years, extensive research has been focused on exploring the behavior and performance of superdense coding in the presence of various types of noisy channels [29–35].

In realistic implementations, decoherence arising from interactions between the quantum system and its environment degrades the entanglement and distinguishability of the encoded states [36, 37], thereby directly reducing the achievable superdense-coding capacity. Overcoming such noise-induced limitations remains a central challenge in the development of reliable and scalable quantum communication networks. Among the various decoherence mechanisms, amplitude damping is of particular importance, as it originates from irreversible energy-relaxation processes and is ubiquitous across a wide range of experimental platforms [38–40]. For example, in optical and trapped-ion qubit systems, spontaneous photon scattering from excited states leads to population decay, significantly affecting the encoded information [41–43]. Unlike Pauli-type noise, amplitude damping cannot be described using Unital operators, which complicates both its analytical treatment and the design of effective protection strategies for superdense-coding protocols. Since any physical evolution of a quantum system can be modeled as a noisy quantum channel, a thorough understanding and mitigation of such noise processes are essential for preserving the information-carrying advantage offered by superdense coding.

Several strategies have been proposed to mitigate the effects of the amplitude damping channel (ADC) in quantum communication protocols, most notably weak measurement–based schemes and environment-assisted measurement (EAM) [44–52]. Weak measurement followed by reversal is commonly employed to suppress decoherence during entanglement distribution; however, its performance strongly depends on the measurement strength and deteriorates significantly in strong decoherence regimes, where it fails to effectively preserve quantum coherence and entanglement. On the other hand, EAM directly addresses channel noise by perform-

* Corresponding author: Muzaffar Qadir Lone; lone.muzaffar@uok.edu.in

ing measurements on the environment and post-selecting system states associated with invertible Kraus operators, followed by conditional recovery operations. While EAM can, in principle, restore the system state probabilistically, it requires direct access to and precise control over the environment, which is experimentally challenging and remains unrealized in current platforms. These inherent limitations of weak measurement and EAM motivate the need for alternative and more practical protection mechanisms, such as the escort qubit protocol proposed in this work, which offers a robust enhancement of superdense coding capacity under ADC.

We present an escort–qubit–assisted scheme for the distribution of entanglement in the presence of an amplitude damping channel (ADC). The central idea of the protocol is to associate an additional auxiliary qubit with each qubit of the entangled pair that propagates through the noisy channel. This auxiliary system, referred to as the *escort qubit*, is initialized in the excited state $|1\rangle$ and is engineered to experience the same environmental noise as its corresponding traveling qubit.

Prior to transmission, each traveling qubit is suitably coupled to its escort qubit via a unitary interaction. This pre–noise coupling correlates the amplitude damping dynamics of the system qubit with that of the escort qubit, thereby providing a mechanism to infer whether a quantum jump has occurred during transmission. After the qubits traverse the ADC, the escort qubit is measured in an appropriate basis to detect the presence or absence of an amplitude damping event. The protocol then post-selects only those runs for which the escort qubit indicates a no-jump trajectory, effectively filtering out error events associated with energy relaxation.

As a result of this conditional measurement and post-selection strategy, the adverse effects of amplitude damping on the shared entanglement can be significantly suppressed. We analyzed three noisy configurations: amplitude damping acting on Alice's qubit, on Bob's qubit, and on both qubits to assess the performance of the proposed escort-assisted superdense coding protocol. The results clearly highlight the effectiveness of the protocol in mitigating ADC-induced decoherence, as it restores the superdense coding capacity to its ideal value of two classical bits regardless of the noise scenario. Moreover, when all ADC trajectories are included, the resulting average capacity, although suboptimal, consistently surpasses the unprotected capacity for all decoherence strengths. Owing to its independence from the specific noise configuration, the proposed protocol can be readily generalized and universalized to multi-qubit superdense coding schemes. From a physical standpoint, the escort qubit can be implemented as an auxiliary photon propagating alongside the system photon through the same optical path or communication channel, thereby ensuring that both qubits experience identical noise dynamics. This common-noise exposure is central to the protocol, as it enables effective mitigation of ADC-induced decoherence without requiring direct access to the environment or conditional measurements. Consequently, the escort–qubit protocol provides a practical and experimentally feasible strategy for protecting entanglement during distribution, further reinforcing its suitability for realistic superdense coding implementations

The remainder of this paper is organized as follows. Section 2 introduces superdense coding in the presence of noisy channels and analyzes three distinct noise configurations: amplitude damping acting on Alice's subsystem, on Bob's subsystem, and on both subsystems. In Section 3, we present the escort-assisted superdense coding protocol for these noisy scenarios and discuss in detail the resulting enhancement in dense-coding capacity. Finally, Section 4 is devoted to the performance analysis of the escort-qubit protocol in optimizing the superdense coding capacity, followed by concluding remarks.

2. SUPERDENSE CODING THROUGH NOISY CHANNELS

In this section, we begin by discussing the superdense coding protocol through amplitude damping channels (ADCs). In all the noisy scenarios, the complete superdense coding protocol consists of four steps: (1) preparation, (2) entanglement distribution, (3) encoding, and (4) decoding, as illustrated in Figs. 1, 2, and 4.

In the first step, the required initial entangled state is prepared. In the second step, Charlie distributes the entangled qubits to Alice and Bob. During this entanglement distribution stage, three distinct noise configurations are considered: (i) in the first case, qubit (a) is sent to Alice through an ADC with decoherence rate γ_a, while qubit (b) is transmitted to Bob through a noiseless channel; (ii) in the second case, qubit (b) is sent to Bob through an ADC with decoherence rate γ_b, whereas qubit (a) is transmitted to Alice through a noiseless channel; and (iii) in the third case, both qubits (a) and (b) are sent through ADCs characterized by decoherence rates γ_a and γ_b, respectively. Upon receiving qubit (a), Alice initiates the third step, which involves the encoding of two classical bits. Specifically, she applies a unitary encoding operation U_k on her qubit, thereby generating the ensemble $\{p_k, \rho_k^\mu\}$, where the superscript $\mu \in \{A, B, AB\}$ labels the noise acting on Alice's subsystem, Bob's subsystem, or both subsystems, respectively. In the final step, after Bob receives the encoded qubit from Alice, he performs appropriate decoding operations to retrieve the classical information.

The performance of the superdense coding protocol in the presence of noise is characterized by the Holevo quantity [23–25], which sets an upper bound on the maximum amount of classical information that can be reliably transmitted to the receiver. For a shared noisy bipartite state ρ_{ab}^n, the Holevo bound is given by

$$\chi_{AD}^{\mu} = S(\rho_{\text{avg}}^{\mu}) - \sum_{k=0}^{3} p_k \, S(\rho_k^{\mu}), \tag{1}$$

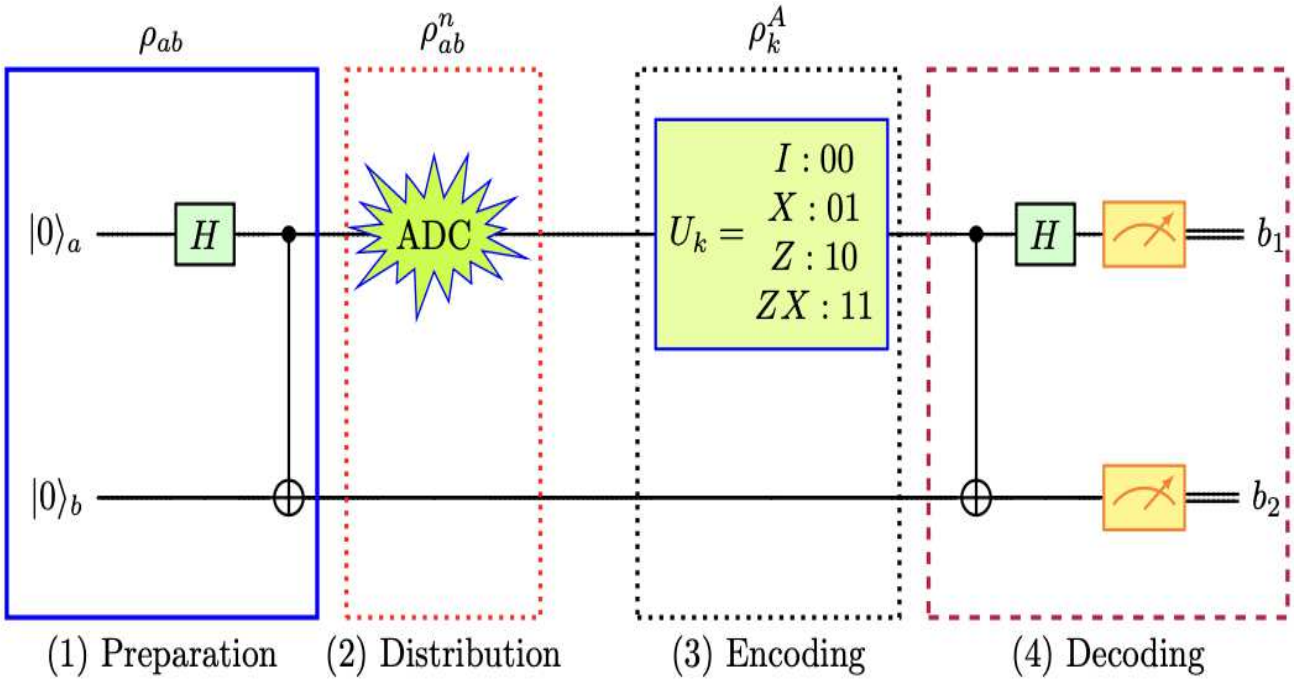


FIG. 1. Quantum circuit of superdense coding when Alices qubit is subjected to AD-noise during entanglement distribution by Charlie. The protocol involves four steps (1) Preparation by Charlie (2) Entanglement distribution by Charlie (3) Alice's unitary encoding and (4) Bob's decoding

where $\rho^{\mu}_{\text{avg}} = \sum_{k=0}^{3} p_k \rho^{\mu}_k$ is the average ensemble state, ρ^{μ}_k denotes the encoded state received by Bob after entanglement distribution and encoding, and $S(\cdot)$ represents the von Neumann entropy.

The superdense coding capacity in the presence of amplitude damping noise is obtained by maximizing the Holevo quantity over all possible encoding probabilities p_k and unitary operations U_k, yielding

$$C^{\mu}_{AD} = \max_{\{p_k, U_k\}} \left[S(\rho^{\mu}_{\text{avg}}) - \sum_{k=0}^{3} p_k \, S(\rho^{\mu}_k) \right]. \tag{2}$$

As shown in [29], when the von Neumann entropy of the encoded states remains invariant under the encoding operations, the optimal superdense coding strategy is achieved by employing unitary Pauli encodings U_k with equal a priori probabilities $p_k = \frac{1}{4}$. This optimal encoding scheme is adopted throughout this work for all noisy configurations $\mu = A, B, AB$ considered in the subsequent subsections.

2.1. Amplitude Damping on Alice's Subsystem

Here, we introduce the superdense coding protocol when Alice's subsytem, interacts with the noisy environment during distribution by Charlie as shown in Fig. 1. In the first step Charlie prepares the entangled channel given by Eq. 3

$$\rho_{\text{ab}} = \frac{1}{2} \begin{pmatrix} 1 & 0 & 0 & 1 \\ 0 & 0 & 0 & 0 \\ 0 & 0 & 0 & 0 \\ 1 & 0 & 0 & 1 \end{pmatrix}. \tag{3}$$

where qubits marked (a) and (b) represent Alice's and Bob's subsytems throughout this paper. During the entanglemnt distribution, Alice's subsytem is passed through an ADC with decoherence rate γ_a and Bob's subsystem through a noiseless channel. This interaction is modelled by a CPTP map by means of operator sum representation. For ADC the map is represented by following Krauss operators.

$$K_0 = \begin{pmatrix} 1 & 0 \\ 0 & e^{-\frac{\gamma t}{2}} \end{pmatrix}, \qquad K_1 = \begin{pmatrix} 0 & \sqrt{1 - e^{-\gamma t}} \\ 0 & 0 \end{pmatrix} \tag{4}$$

where γ is the decoherence rate. The amplitude damping channel is employed to model energy dissipation during entanglement distribution. The corresponding Kraus operators are expressed in terms of the decay parameter γt, which captures the exponential loss of excitation arising from Markovian system–environment interactions. This representation enables a transparent, time-dependent analysis of decoherence effects on the superdense coding capacity.

The state recieved by the two partners once Charlie sends qubit (a) through ADC with decoherence rate γ_a

and qubit (b) through noiseless channel is

$$\rho_{ab}^{n} = \sum_{i=0}^{1} \left(K_i^{(a)} \otimes I^{(b)}\right) \rho_{ab} \left(K_i^{(a)} \otimes I^{(b)}\right)^{\dagger} = \frac{1}{2} \begin{pmatrix} 1 & 0 & 0 & e^{-\frac{\gamma_a t}{2}} \\ 0 & 1-e^{-\gamma_a t} & 0 & 0 \\ 0 & 0 & 0 & 0 \\ e^{-\frac{\gamma_a t}{2}} & 0 & 0 & e^{-\gamma_a t} \end{pmatrix}. \tag{5}$$

After the entanglement distribution, Alice encodes two classical bits on her qubit (a) by applying one of the unitary operations U_k $(k = 0, 1, 2, 3)$ with equal probability $p_k = \frac{1}{4}$. This choice of equal a priori probabilities is optimal for superdense coding. The encoded ensemble that Bob recieves is $\{p_k = \frac{1}{4}, \rho_k^A; (\mu = A)\}$, with ρ_k^A being the encoded state recieved by Bob and is given by

$$\rho_k^A = \left(U_k^{(a)} \otimes I^{(b)}\right) \rho_{\mathrm{ab}}^{n} \left(U_k^{(a)\dagger} \otimes I^{(b)}\right) \tag{6}$$

where $U_k^{(a)} = I : k = 0, \sigma_x : k = 1, \sigma_z : k = 2$ and $\sigma_z\sigma_x : k = 3$. After receiving the encoded qubit, Bob decodes the classical information using appropriate decoding operations, as shown in Fig. 1. The superdense coding capacity given by Eq. 2 ,for the present case $(\mu = A)$ takes the form

$$C_{\mathrm{AD}}^{A} = S(\rho_{\mathrm{avg}}^{A}) - \sum_{k=0}^{3} p_k S(\rho_{\mathrm{k}}^{A}) \tag{7}$$

where $S(.)$ is the von Neumann entropy and ρ_{avg}^{A} is the average matrix of the ensemble $\{p_k = \frac{1}{4}, \rho_k^A\}$ given by

$$\rho_{\mathrm{avg}}^{A} = \sum_{k=0}^{3} p_k \rho_k^A = \frac{I_{4\times 4}}{4} \tag{8}$$

Moreover, since the unitary operations U_k correspond to pure rotations, they do not modify the eigenvalue spectrum of the encoded states. Consequently, the von Neumann entropy remains identical for all encoded states, and the channel capacity given by Eq. 7 reduces to the following form.

$$C_{\mathrm{AD}}^{A} = S(\rho_{\mathrm{avg}}^{A}) - S(\rho_{\mathrm{k}}^{A}) \tag{9}$$

To illustrate the destructive effect of the amplitude damping channel (ADC), the channel capacity given by Eq. 9 is plotted in Fig. 3(a) as a function of the dimensionless decoherence parameter γt, with $\gamma_a = \gamma$. As evident from Fig. 3(a), an increase in the decoherence strength γt during the entanglement distribution leads to a monotonic decrease in the channel capacity C_{AD}^{A} over time. The maximum capacity $C_{\mathrm{AD}}^{A} = 2$ is attained only in the absence of decoherence, i.e., when $\gamma t = 0$, which corresponds to the ideal superdense coding scenario. It is evident that $C_{\mathrm{AD}}^{A} \geq 1$ in the strong decoherence regime, as the unitary encodings symmetrically redistribute the effects of the ADC and partially preserve the distinguishability of the encoded states.

2.2. Amplitude Damping on Bob's Subsystem

In this subsection we discuss the noisy scenario when Bob's subsystem is passed through ADC having decoherence rate γ_b and that of Alice through a noiseless channel as shown in Fig. 2. Charlie again prepares the bell state given by Eq. 3, however now sends the qubit (b) to Bob through ADC and qubit (a) through noise free channel to Alice. Now the state after entanglement distribution is

$$\rho_{ab}^{n'} = \sum_{j=0}^{1} \left(I^{(a)} \otimes K_j^{(b)}\right) \rho_{ab} \left(I^{(a)} \otimes K_j^{(b)}\right)^{\dagger} = \frac{1}{2} \begin{pmatrix} 1 & 0 & 0 & e^{-\frac{\gamma_b t}{2}} \\ 0 & 0 & 0 & 0 \\ 0 & 0 & 1-e^{-\gamma_b t} & 0 \\ e^{-\frac{\gamma_b t}{2}} & 0 & 0 & e^{-\gamma_b t} \end{pmatrix}. \tag{10}$$

Alice encodes using unitary encoding operationa U_k on her qubit (a) and sends the encoded qubit to Bob. The ensemble at Bob's place is $\{p_k = \frac{1}{4}, \rho_k^B; \mu = B\}$, with ρ_k^B given by

$$\rho_k^B = \left(U_k^{(a)} \otimes I^{(b)}\right) \rho_{\mathrm{ab}}^{n'} \left(U_k^{(a)\dagger} \otimes I^{(b)}\right) \tag{11}$$

Now, the superdense coding capacity given in Eq. 2 for the present case $(\mu = B)$ takes the form

$$C_{\mathrm{AD}}^{B} = S(\rho_{\mathrm{avg}}^{B}) - \sum_{k=0}^{3} p_k S(\rho_{\mathrm{k}}^{B}) \tag{12}$$

where the superscript indicates the noise on Bob's qubit and the ensemble average matrix takes the form

$$\rho_{\mathrm{avg}}^{B} = \sum_{k=0}^{3} p_k \rho_k^B = \frac{1}{4} \begin{pmatrix} 2-e^{-\gamma_b t} & 0 & 0 & 0 \\ 0 & e^{-\gamma_b t} & 0 & 0 \\ 0 & 0 & 2-e^{-\gamma_b t} & 0 \\ 0 & 0 & 0 & e^{-\gamma_b t} \end{pmatrix}. \tag{13}$$

Now due to invariance of von Neumann entropy under unitary transformations Eq. 12 reduces to

$$C_{\mathrm{AD}}^{B} = S(\rho_{\mathrm{avg}}^{B}) - S(\rho_{\mathrm{k}}^{B}) \tag{14}$$

The superdense coding capacity strongly depends on both the degree of entanglement of the shared resource state and the distinguishability of the encoded states at the decoding stage of the protocol. The capacity C_{AD}^{B}, given by Eq. 14, is plotted as a function of the decoherence strength γt with $\gamma_b = \gamma$ in Fig. 3(b). It is evident that noise acting on Bob's qubit has a more adverse effect on the channel capacity than noise acting on Alice's qubit, as demonstrated in Fig. 3. In the strong decoherence regime, the superdense coding capacity falls

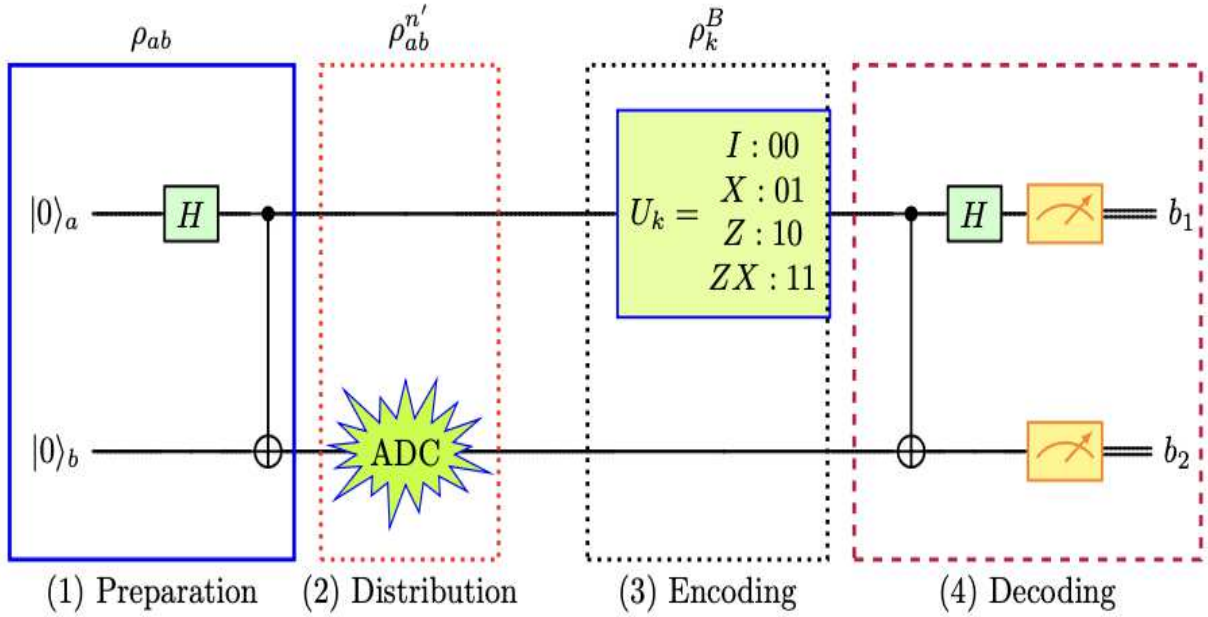


FIG. 2. Quantum circuit of superdense coding when Bob's qubit is subjected to AD-noise during entanglement distribution by Charlie.

below the classical limit of one bit. This behavior can be attributed to the fact that the unitary encoding operations performed on the noiseless qubit do not symmetrize the effects of the amplitude damping channel, leading to a significant loss of distinguishability among the encoded states. Furthermore, the capacity attains its maximum value of $C_{\rm AD}^B = 2$ only in the absence of decoherence (i.e., $\gamma t = 0$), corresponding to the ideal superdense coding scenario. These results clearly indicate that the ADC effects render the shared entangled state impractical for superdense coding in realistic environments, thereby necessitating the implementation of suitable protection schemes to counteract decoherence and enhance the channel capacity.

2.3. Amplitude Damping on Both Subsystems

The most general noise scenario where both Alice and Bob's subsytems are subjected to decoherence during entanglement distribution by Charlie is discussed in this subsection and schematically represented in Fig. 4. The ADC's respectively have decoherence rates γ_a and γ_b acting independently on qubits (a) and (b). After the entanglement distribution step the noisy state shared between the two partners is given by Eq. 15

$$\rho_{ab}^{n''} = \sum_{i,j=0}^{1} \left(K_i^{(a)} \otimes K_j^{(b)}\right) \rho_{ab} \left(K_i^{(a)} \otimes K_j^{(b)}\right)^\dagger$$
$$= \frac{1}{2} \begin{pmatrix} 1+(1-e^{-\gamma_a t})(1-e^{-\gamma_b t}) & 0 & 0 & e^{-\frac{\gamma_a+\gamma_b}{2}t} \\ 0 & e^{-\gamma_b t}(1-e^{-\gamma_a t}) & 0 & 0 \\ 0 & 0 & e^{-\gamma_a t}(1-e^{-\gamma_b t}) & 0 \\ e^{-\frac{\gamma_a+\gamma_b}{2}t} & 0 & 0 & e^{-(\gamma_a+\gamma_b)t} \end{pmatrix}. \quad (15)$$

Alice encodes using the same set of unitary operatons on her subsystem as in the above two noisy scenarios and as shown in the encoding step in Fig. 4. With an equal apriori probability of $p_k = \frac{1}{4}$, the ensemble at Bob's side

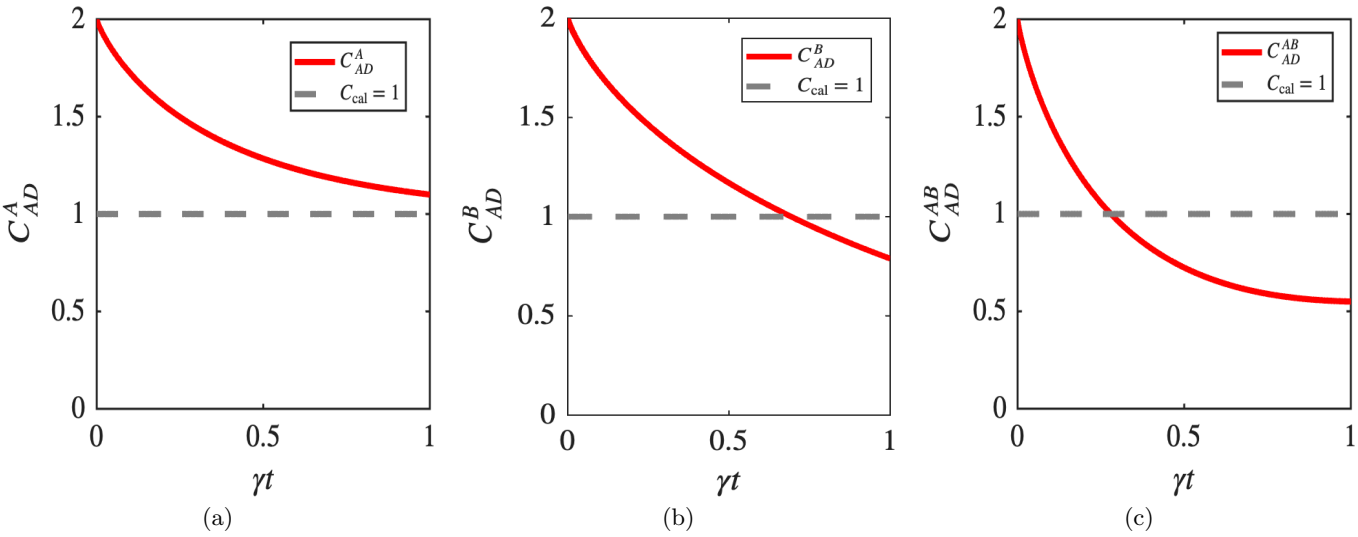


FIG. 3. Superdense coding capacity as a function of the dimensionless decoherence parameter γt under amplitude damping noise. Fig. 3(a) shows capacity $C^A_{\rm AD}$ when only Alice's subsystem is passed through the amplitude damping channel during entanglement distribution. Fig. 3(b) illustrates capacity $C^B_{\rm AD}$ when only Bob's subsystem is subjected to noise. Fig. 3(c) capacity $C^{AB}_{\rm AD}$ when both subsystems interact with the noisy environment, with $\gamma_a = \gamma_b = \gamma$. The horizontal line denotes the classical capacity limit $C_{\rm cal} = 1$.

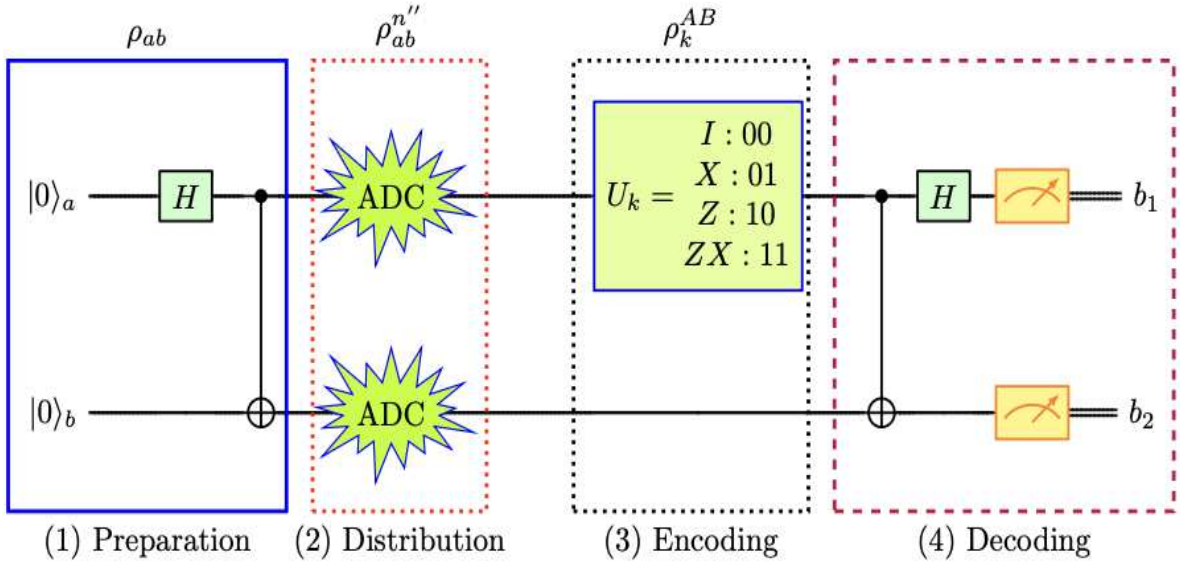


FIG. 4. Quantum circuit of superdense coding when both qubits are subjected to AD-noise during entanglement distribution by Charlie.

after reciveving the encoded qubit from Alice is $\{p_{\rm k} = \frac{1}{4}, \rho^{AB}_{\rm k}; \mu = AB\}$, and the state $\rho^{AB}_{\rm k}$ is given by

$$\rho^{AB}_{\rm k} = \left(U^{(a)}_k \otimes I^{(b)}\right) \rho^{n''}_{\rm ab} \left(U^{(a)\dagger}_k \otimes I^{(b)}\right) \tag{16}$$

also the superdense coding capacity following the similar notation as in Eqs. 7 and 12, takes the form

$$C^{AB}_{\rm AD} = S(\rho^{AB}_{\rm avg}) - \sum_{k=0}^{3} p_k S(\rho^{AB}_{\rm k}) \tag{17}$$

with the superscript depicting the noise on both subsystems and the ensemble average matrix considering equal probability (i.e $p_k = \frac{1}{4}$) reduces to

$$\rho_{\text{avg}}^{AB} = \sum_{k=0}^{3} p_k \rho_k^{AB} = \frac{1}{4}\begin{pmatrix} 2 - e^{-\gamma_b t} & 0 & 0 & 0 \\ 0 & e^{-\gamma_b t} & 0 & 0 \\ 0 & 0 & 2 - e^{-\gamma_b t} & 0 \\ 0 & 0 & 0 & e^{-\gamma_b t} \end{pmatrix} \tag{18}$$

the channel capacity given in Eq. 17 considering the independence of von Neumann entropy on encoding Pauli operations U_k takes the form

$$C_{\text{AD}}^{AB} = S(\rho_{\text{avg}}^{AB}) - S(\rho_{\text{k}}^{AB}) \tag{19}$$

The channel capacity C_{AD}^{AB}, given by Eq. 19, is plotted in Fig. 3(c) by assuming that both qubits, during the distribution stage, are transmitted through independent ADC's with identical decoherence rates, i.e., $\gamma_a = \gamma_b = \gamma$. It is observed that the channel capacity undergoes a most strongest decay among the three noise scenarios due to a combined ADC effects on both the qubits. Moreover its observed that the channel capcity falls below the classical limit at smaller decoherence strengths. The decrease in capacity arises from the rapid suppression of quantum coherence and entanglement due to amplitude damping, which leads to a reduced distinguishability among the encoded states. A monotonic decrease in capacity is observed with the increase in amplitude damping strength. Due to combined ADC effects the capacity C_{AD}^{AB} falls below the classical limit $C_{cal} = 1$ even at smaller decoherence strengths, marking the complete loss of quantum advantage.

From the superdense coding capacities given in Eqs. 9, 14, and 19, and illustrated in Fig. 3 for the three noisy scenarios, it is evident that the effects of the amplitude damping channel severely degrade both the entanglement of the shared resource state and the distinguishability of the encoded ensemble. As a consequence, the superdense coding capacity undergoes a rapid decay, leading to a loss of quantum advantage. This clearly highlights the necessity of implementing appropriate protection strategies to counteract the adverse effects of amplitude damping and to enhance the channel capacity.

3. ESCORTING QUBIT PROTOCOL

In this section, we describe our escort-qubit-assisted protocol for the distribution of entanglement in the presence of an amplitude damping channel (ADC). The essential idea of the scheme is to associate an additional auxiliary qubit with each qubit of the entangled pair that propagates through the noisy environment. This auxiliary system, termed the *escort qubit*, is initialized in the excited state $|1\rangle$ and is arranged to undergo the same noise dynamics as its corresponding resource qubit. The escort-qubit protocol is demonstrated in Fig. 5, 8 and 11 and proceeds through the following stages:

a. Escort-assisted state preparation A third party charlie acts as a controller of the proposed escort-qubit protocol as illusttrated in Figs. 5, 8 and 11. Before the entangled qubits are distributed to respective partners through ADC's, the controller prepares an escort in state $|1\rangle$ for every entangled qubit that goes through an ADC. A controlled-NOT (CNOT) gate is applied between the qubit-escort pair with qubit as control, while the escort as the target. This operation correlates the information of the traveling qubit with the auxiliary system to keep track of flip and no-flip trajectories.

b. Escort-based recovery and measurement Once the qubits have propagated through their respective ADC's and are received at the destination nodes, the decoupling CNOT operation is applied again as in the initial stage, the qubit from the entangled pair is used as the control and the escort qubit as the target. This decoding operation aims to reverse the effect of the pre-noise coupling and redistribute the noise information onto the escort qubits. Each receiver then performs a projective measurement on the escort qubit in the computational basis. By post-selecting the no-flip trajectories which coresponds to a measurement outcome of $|1\rangle$ for each escort, the shared state between two nodes is projected to the original maximally entangled state. Outcomes corresponding to other measurement results are discarded. Afterwards Alice and Bob perform the standard encoding and decoding steps of the superdense coding with a maximally entangled state as a resource and achieves the ideal superdense coding capacity of two bits. Experimentally, the escort qubit can be implemented using an auxiliary photon that co-propagates with the resource photon through the same optical path. With the current level of technological advancement in photonic platforms, this scheme is experimentally feasible and constitutes a practical approach for suppressing decoherence effects. The escort-qubit protocol for the three noisy configurations is disscussed below.

3.1. Escorting Qubit Protocol with Amplitude Damping on Alice's Subsystem

Here, we discuss the proposed escort qubit protocol when only Alice's qubit is passing through ADC. Charlie prepares the bell state along with an escort in state $|1\rangle_{e_a}$ as shown in Fig. 5. Also a CNOT gate operation is applied between the qubit-escort pair $\big((a), e_a\big)$ to couple them. The state of the three qubits takes the form

$$\rho_{abe_a} = \frac{1}{2}\Big[(|001\rangle + |110\rangle)(\langle 001| + \langle 110|)\Big] \tag{20}$$

Both the entangled qubit and its escort are distributed to Alice through an ADC with decoherence rate γ_a. The

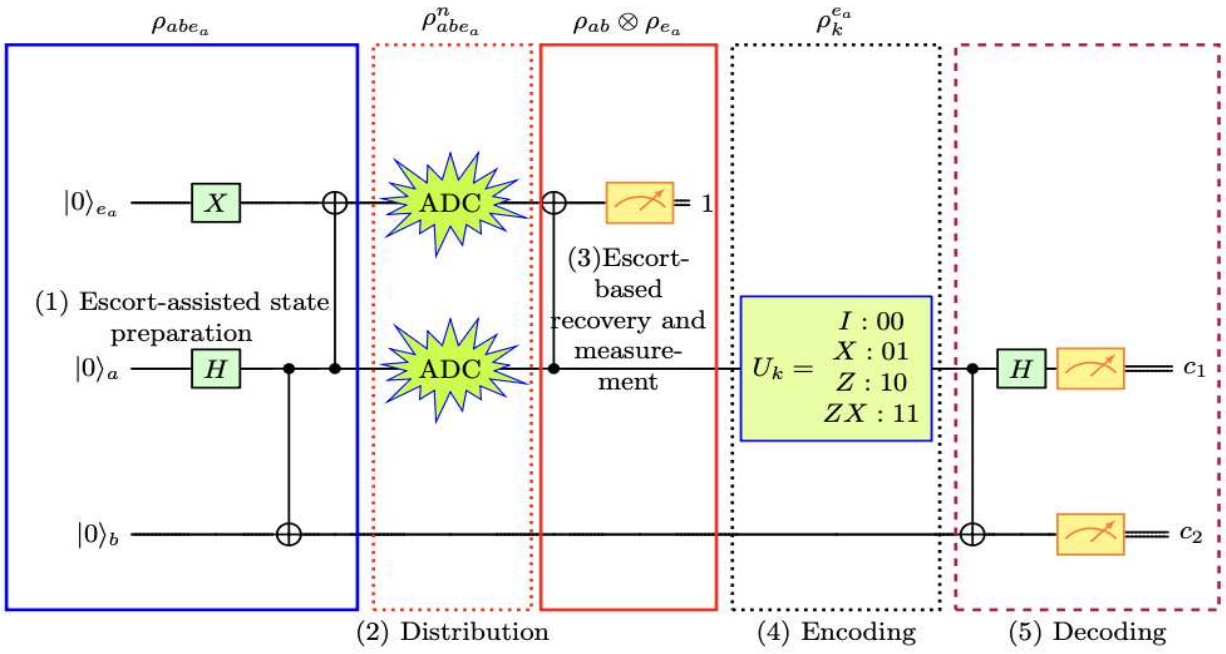


FIG. 5. Quantum circuit of optimized superdense coding by escorting Alice's noisy qubit and post selecting no flip trajectory for perfect superdense coding.

other entangled qubit is sent to Bob through a noiseless channel and the noisy shared state becomes

$$\begin{aligned}\rho^n_{abe_a} &= \sum_{i,i'=0}^{1} \left(K_i^{(a)} \otimes I \otimes K_{i'}^{(e_a)}\right) \rho_{abe_a} \left(K_i^{(a)} \otimes I \otimes K_{i'}^{(e_a)}\right)^\dagger \\ &= \frac{1}{2}\Big[e^{-\gamma_a t}\left(|001\rangle + |110\rangle\right)\left(\langle 001| + \langle 110|\right) \\ &+ \left(1 - e^{-\gamma_a t}\right)\left(|000\rangle\langle 000| + |010\rangle\langle 010|\right)\Big].\end{aligned} \tag{21}$$

where $K_{i,j}$ are defined in Eq. 4. Also after the decoupling CNOT gate operation between the noisy qubit-escort pair the joint state becomes

$$\begin{aligned}\rho^n_{ab} \otimes \rho_{e_a} = \frac{1}{2}\Big[&e^{-\gamma_a t}\left(|00\rangle + |11\rangle\right)\left(\langle 00| + \langle 11|\right) \otimes |1\rangle\langle 1| \\ &+ \left(1 - e^{-\gamma_a t}\right)\left(|00\rangle\langle 00| + |01\rangle\langle 01|\right) \otimes |0\rangle\langle 0|\Big].\end{aligned} \tag{22}$$

By measuring and post selecting the escort in the computational basis state $|1\rangle_{e_a}$, the shared state between the two nodes is projected onto a maximally entangled bell state and is obtained by tracing out the escort.

$$\begin{aligned}\rho_{\mathrm{ab}} &= \frac{\mathrm{Tr}_{e_a}(\rho^n_{ab} \otimes \rho_{e_a})_{|1\rangle}}{W^{e_a}} \\ &= \frac{1}{2W^{e_a}}\Big[e^{-\gamma_a t}\left(|00\rangle + |11\rangle\right)\left(\langle 00| + \langle 11|\right)\Big]\end{aligned} \tag{23}$$

where W^{e_a} is the success probability of escort qubit protocol with noise on Alice's subsytem only and is given by

$$W^{e_a} = e^{-\gamma_a t} \tag{24}$$

After succesfully restoring the shared state to a maximally entangled bell state Alice and Bob follow the usual encoding and decoding steps of superdense coding. Now with a maximally entangled bell state as a resource for superdense coding the capacity is enhanced probabilistically to its optimum value given below

$$C^{e_a}_{AD} = 2 \tag{25}$$

To assess the effectiveness of the proposed escort-assisted superdense coding protocol in enhancing the channel capacity, we examine the behavior of the enhanced capacity, defined as the difference between the capacities achieved with and without the escort qubit.

$$C^A_{en} = C^{e_a}_{AD} - C^A_{AD} \tag{26}$$

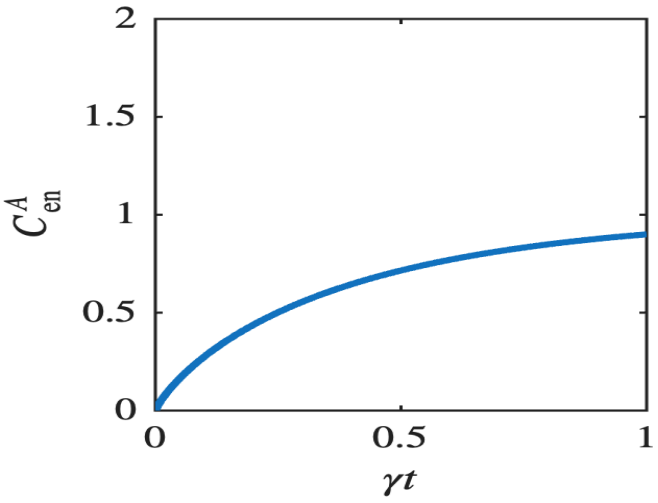


FIG. 6. Enhancement in superdense coding capacity C^A_{en} as a function of the decoherence parameter γt with $\gamma_a = \gamma$. In the strong decoherence regime, the enhancement approaches unity showing complete suppression of ADC effects.

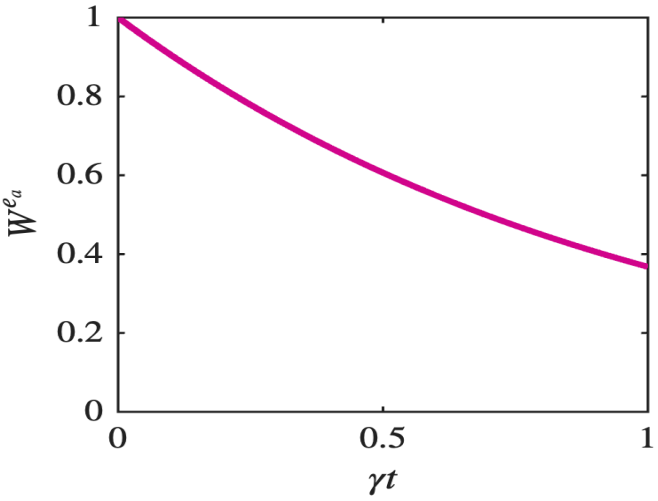


FIG. 7. Success probability of the escort qubit protocol as a function of γt, clearly the protocol enhances the capacity with high probability.

with C^A_{AD} given by Eq. 9 and illustrated in Fig. 3(a). Also the enhanced capacity C^A_{en} given in Eq. 26 and the corresponding success probability given by Eq. 24 are plotted in Fig. 6 and Fig. 7 respectively. It is clear that the proposed escort qubit assisted superdense coding protocol remarkably enhances the capacity for all decoherence regimes and interaction times with a non zero probability. In the strong decoherence regime where the ADC effects are most adverse the enhancement in capacity $C^A_{en} \sim 1$, indicating a complete suppression of decoherence during entanglement distribution.

3.2. Escorting Qubit Protocol with Amplitude Damping on Bob's Subsystem

In this subsection, we discuss the effectiveness of the proposed escort qubit protocol when Bob's subsystem is subjected to noise during entanglement distribution. The complete protocol is shown in Fig. 8, where Charlie initialises the protocol by preparing the Bell state and the escort in state $|1\rangle_{e_b}$. Aftter pre-noise CNOT operation between entangled qubit and its escort the state becomes

$$\rho_{abe_b} = \frac{1}{2}\Big[(|001\rangle + |110\rangle)(\langle 001| + \langle 110|)\Big] \tag{27}$$

Now, Charlie sends the qubit (b) and its escort (e_b) thorugh ADC with decoherence rate γ_b and the post distribution state becomes

$$\begin{aligned}\rho^n_{abe_b} &= \sum_{j,j'=0}^{1}\left(I\otimes K^{(b)}_j\otimes K^{(e_b)}_{j'}\right)\rho_{abe_b}\left(I\otimes K^{(b)}_j\otimes K^{(e_b)}_{j'}\right)^\dagger \\ &= \frac{1}{2}\Big[e^{-\gamma_b t}\left(|001\rangle + |110\rangle\right)\left(\langle 001| + \langle 110|\right) \\ &\quad + \left(1-e^{-\gamma_b t}\right)\left(|000\rangle\langle 000| + |100\rangle\langle 100|\right)\Big]\end{aligned} \tag{28}$$

Subsequently, after applying the decoupling CNOT gate operation between the noisy qubit-escort pair $\big((b), e_b\big)$, the joint state becomes

$$\begin{aligned}\rho^n_{ab}\otimes\rho_{e_b} = \frac{1}{2}\Big[&e^{-\gamma_b t}\left(|00\rangle + |11\rangle\right)\left(\langle 00| + \langle 11|\right)\otimes|1\rangle\langle 1| \\ &+ \left(1-e^{-\gamma_b t}\right)\left(|00\rangle\langle 00| + |10\rangle\langle 10|\right)\otimes|0\rangle\langle 0|\Big].\end{aligned} \tag{29}$$

Again by measuring the escort in the computational basis state $|1\rangle_{e_b}$ the no flip trajectory is obtained and the state of the two qubits is restored to a maximally entangled Bell state. This state is obtained by tracing out escort as

$$\begin{aligned}\rho_{\text{ab}} &= \frac{\text{Tr}_{e_b}(\rho^n_{ab}\otimes\rho_{e_b})_{|1\rangle}}{W^{e_b}} \\ &= \frac{1}{2W^{e_b}}\Big[e^{-\gamma_b t}\left(|00\rangle + |11\rangle\right)\left(\langle 00| + \langle 11|\right)\Big]\end{aligned} \tag{30}$$

where W^{e_b} is the success probability of escort qubit protocol with noise on Bob's subsytem only and is given by

$$W^{e_b} = e^{-\gamma_b t} \tag{31}$$

Once the shared quantum state has been successfully recovered to a maximally entangled Bell state despite the presence of noise on Bob's side, Alice and Bob proceed with the standard encoding and decoding operations of

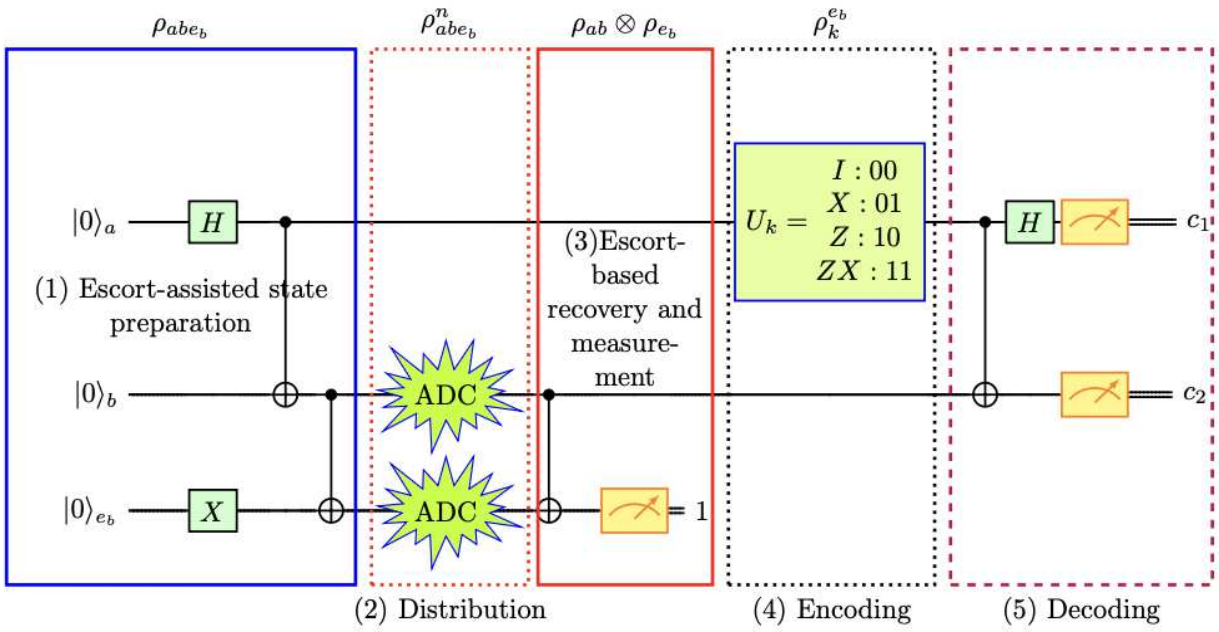


FIG. 8. Quantum circuit of optimized superdense coding by escorting Bobs's noisy qubit and post selecting no flip trajectory for perfect superdense coding.

the superdense coding protocol. When a maximally entangled Bell pair is available as the communication resource, the superdense coding capacity can be probabilistically restored to its optimal value given by

$$C^{e_b}_{AD} = 2. \tag{32}$$

To quantitatively evaluate the performance of the proposed escort-assisted superdense coding scheme under Bob's noise, we again observe the behaviour of enhancement in capacity which is given by

$$C^B_{en} = C^{e_b}_{AD} - C^B_{AD}. \tag{33}$$

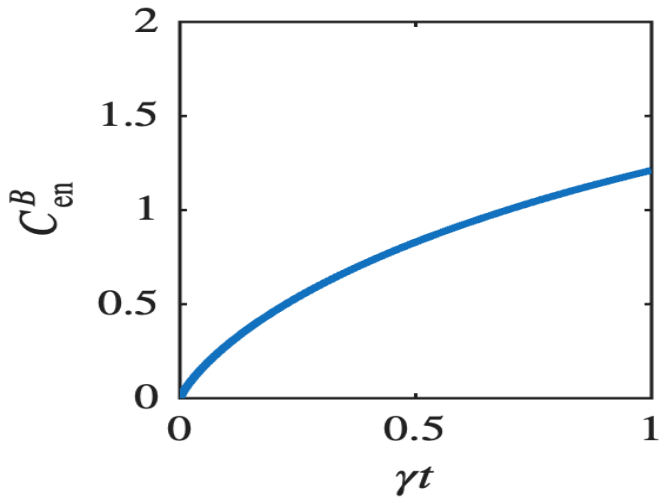


FIG. 9. Enhanced superdense coding capacity C^B_{en} as a function of the decoherence parameter γt with $\gamma_b = \gamma$.

where C^B_{AD} given by Eq. 14. The enhancement in capacity serves as a quantitative measure of the operational benefit provided by the escort-assisted recovery procedure, indicating the extent to which classical information transmission can be restored despite the presence of noise on Bob's qubit. The behavior of this enhanced capacity is illustrated in Fig. 9, while the corresponding success probability of the protocol is shown in Fig. 10. The be-

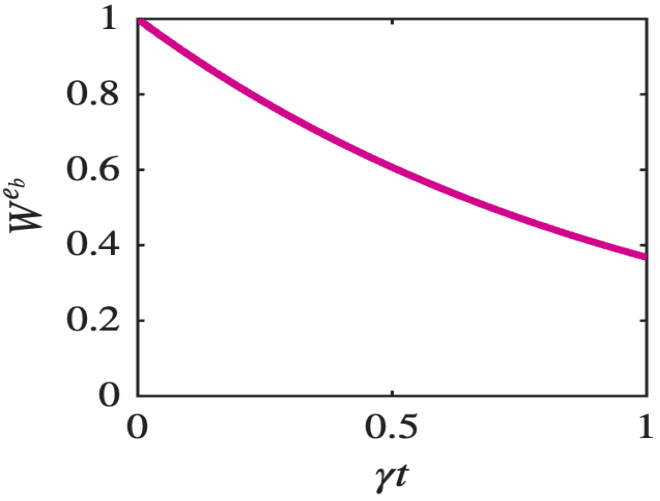


FIG. 10. Success probability of the escort qubit protocol as a function of γt, clearly the protocol strongly suppreses the noise with high probability.

havior of the enhanced capacity C^B_{en} clearly demonstrates that the escort-qubit–assisted protocol leads to an improvement in the superdense coding capacity across the entire range of decoherence parameters, with a high probability of success. Moreover, as the strength of the amplitude damping channel increases, the advantage of the proposed scheme becomes more pronounced, as reflected by the corresponding growth of C^B_{en}.

3.3. Escorting Qubit Protocol with Amplitude Damping on Both Subsystems

This subsection addresses the general noise scenario in which both Alice's and Bob's subsystems are affected by ADC's, and examines the application of the escort-qubit–assisted protocol for mitigating the resulting decoherence effects. The quantum circuit of the proposed protocol is shown in Fig. 11 and proceeds with Charlie preparing the resource state given by Eq. 3 and the corresponding escorts in state $|1\rangle_{e_a}$ and $|1\rangle_{e_b}$. After applying the CNOT gate between the resource qubit and its escort prior to the onset of noise yields the following four-qubit joint state:

$$\rho_{abe_ae_b} = \frac{1}{2}\Big[(|0011\rangle + |1100\rangle)(\langle 0011| + \langle 1100|)\Big] \quad (34)$$

Next, the resource qubit (a) along with its escort e_a is transmitted to Alice through an ADC with decoherence rate γ_a, while the resource qubit (b) and its escort e_b are sent to Bob via an ADC with decoherence rate γ_b. The resulting noisy state after the entanglement distribution can be expressed as

$$\begin{aligned}\rho^n_{abe_ae_b} &= \sum_{i,j,i',j'=0}^{1}\Big(K_i^{(a)}\otimes K_j^{(b)}\otimes K_{i'}^{(e_a)}\otimes K_{j'}^{(e_b)}\Big)\rho_{abe_ae_b}\\ &\quad\times\Big(K_i^{(a)}\otimes K_j^{(b)}\otimes K_{i'}^{(e_a)}\otimes K_{j'}^{(e_b)}\Big)^\dagger\\ &= \frac{1}{2}\Big[e^{-(\gamma_a+\gamma_b)t}\left(|0011\rangle + |1100\rangle\right)\left(\langle 0011| + \langle 1100|\right)\\ &\quad + e^{-\gamma_a t}\big(1-e^{-\gamma_b t}\big)\left(|0010\rangle\langle 0010| + |1000\rangle\langle 1000|\right)\\ &\quad + e^{-\gamma_b t}\big(1-e^{-\gamma_a t}\big)\left(|0001\rangle\langle 0001| + |0100\rangle\langle 0100|\right)\\ &\quad + 2\big(1-e^{-\gamma_a t}\big)\big(1-e^{-\gamma_b t}\big)|0000\rangle\langle 0000|\Big]\end{aligned} \quad (35)$$

where $\mathrm{Tr}(\rho^n_{abe_ae_b}) = 1$, showing the map is trace preserving. Now after the decoupling CNOT gate operations on the noisy resource qubit and its escort the state becomes

$$\begin{aligned}&\rho^n_{ab}\otimes\rho_{e_ae_b} =\\ &\frac{1}{2}\Big[e^{-(\gamma_a+\gamma_b)t}\left(|00\rangle + |11\rangle\right)\left(\langle 00| + \langle 11|\right)\otimes|11\rangle\langle 11|\\ &\quad + e^{-\gamma_a t}\big(1-e^{-\gamma_b t}\big)\left(|00\rangle + |10\rangle\right)\left(\langle 00| + \langle 10|\right)\otimes|10\rangle\langle 10|\\ &\quad + e^{-\gamma_b t}\big(1-e^{-\gamma_a t}\big)\left(|00\rangle + |01\rangle\right)\left(\langle 00| + \langle 01|\right)\otimes|01\rangle\langle 01|\\ &\quad + 2\big(1-e^{-\gamma_a t}\big)\big(1-e^{-\gamma_b t}\big)\left(|00\rangle\langle 00|\right)\otimes|00\rangle\langle 00|\Big]\end{aligned} \quad (36)$$

Now, both the partners measure their escorts in computational basis and retain the measurement outcome $|11\rangle_{e_ae_b}$. This corresponds to the no flip trajectory and the shared resource state between them is projected to a maximally entangled state given by

$$\begin{aligned}\rho_{\mathrm{ab}} &= \frac{\mathrm{Tr}_{e_ae_b}(\rho^n_{ab}\otimes\rho_{e_ae_b})_{|1\rangle}}{W^{e_ae_b}}\\ &= \frac{1}{2W^{e_ae_b}}\Big[e^{-(\gamma_a+\gamma_b)t}\left(|00\rangle + |11\rangle\right)\left(\langle 00| + \langle 11|\right)\Big]\end{aligned} \quad (37)$$

where $W^{e_ae_b}$ is the success probability of escort qubit protocol with noise on both subsytems and is given by

$$W^{e_ae_b} = e^{-(\gamma_a+\gamma_b)t} \quad (38)$$

After successfully establishing a maximally entangled state between the two nodes with success probability $W^{e_ae_b}$, Alice encodes two classical bits via Pauli operations, which are subsequently decoded by Bob. Consequently, the escort qubit protocol maximizes the superdense coding capacity to

$$C^{e_ae_b}_{AD} = 2. \quad (39)$$

Again for assessing the performance of the escort-assisted superdense coding protocol when both Alice's and Bob's

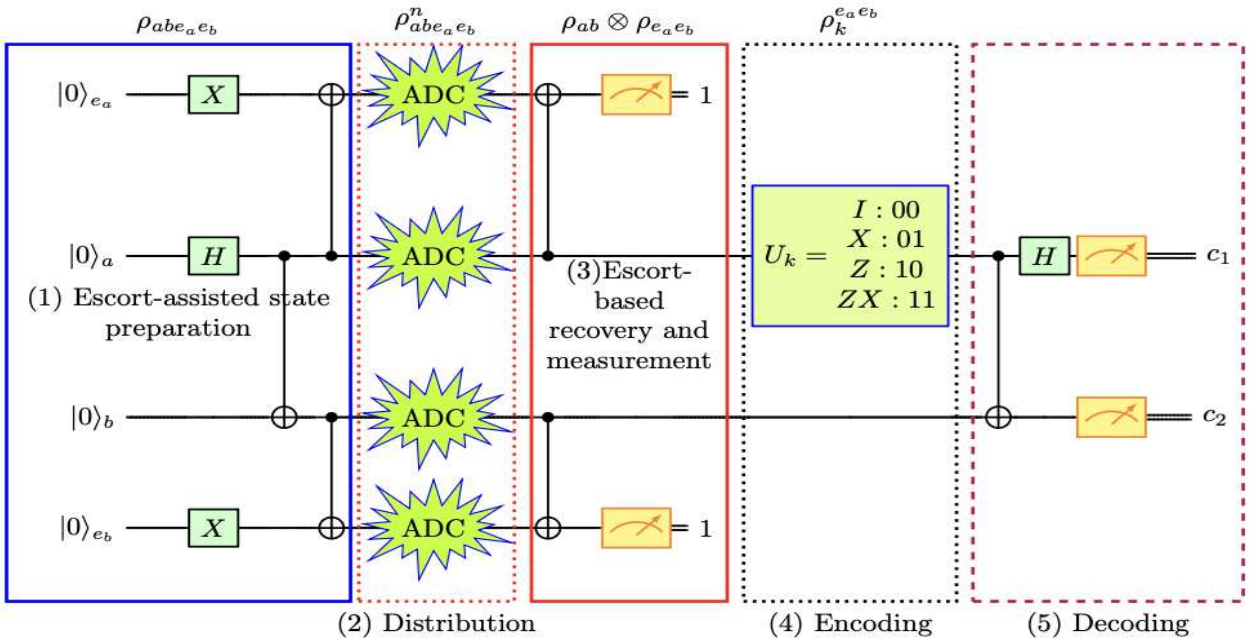


FIG. 11. Quantum circuit of optimized superdense coding by escorting both noisy qubits and post selecting no flip trajectory for perfect superdense coding.

qubits are affected by amplitude damping, we examine the enhancement in capacity defined as

$$C_{en}^{AB} = C_{AD}^{e_ae_b} - C_{AD}^{AB}, \tag{40}$$

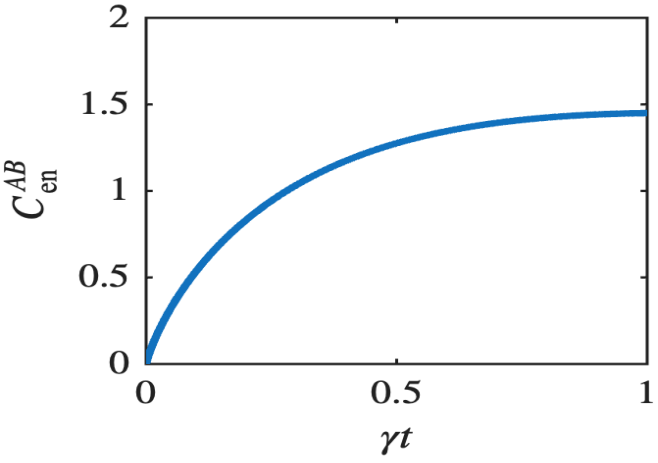


FIG. 12. Enhancement in superdense coding capacity C_{en}^{AB} as a function of the decoherence parameter γt with $\gamma_a = \gamma_b = \gamma$.

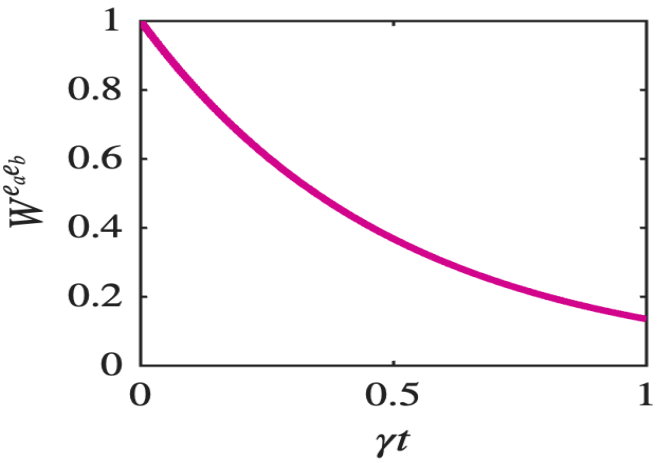


FIG. 13. Success probability of the escort qubit protocol as a function of γt, clearly the protocol optimizes the capacity with non-zero probability

where C_{AD}^{AB} denotes the standard superdense coding capacity in the presence of amplitude damping on both qubits. The behavior of the enhanced capacity is presented in Fig. 12, with the corresponding success probability of the protocol shown in Fig. 13.

Fig. 12 illustrates the enhancement in superdense coding capacity, C_{en}^{AB}, and the corresponding success probability $W^{e_ae_b}$ as functions of the dimensionless decoherence parameter γt. As shown in Fig. 12, the capacity en-

hancement increases monotonically with γt. In the weak decoherence regime, the advantage of the escort-qubit protocol is marginal, whereas for stronger noise the unprotected capacity rapidly degrades while the escorted protocol efficiently preserves high-fidelity entanglement through post-selection of no-jump trajectories. Consequently, a significant enhancement in the superdense coding capacity is observed even at large γt. Fig 13 shows that the success probability $W^{e_a e_b}$ decreases monotonically with increasing γt, reflecting the growing likelihood of amplitude damping events. Together, these results highlight the intrinsic trade-off of the escort-qubit protocol: higher capacity enhancement is achieved at the expense of a reduced success probability, which is a characteristic feature of probabilistic noise-mitigation schemes.

4. DISCUSSION AND CONCLUSION

In this paper, we propose an escort-qubit protocol to optimize the superdense coding capacity in the presence of amplitude damping channel (ADC) effects. We analyze three distinct noisy scenarios, namely amplitude damping acting on Alice's subsystem, on Bob's subsystem, and on both subsystems. The behavior of the superdense coding capacity is examined for each of these cases, and it is observed that the capacity decreases monotonically with increasing values of the dimensionless decoherence parameter γt, as illustrated in Fig. 3. Furthermore, in the strong decoherence regime, the capacity is found to fall below the classical limit $C_{\rm cal} = 1$, indicating a complete loss of quantum advantage and thereby necessitating the implementation of an effective mitigation strategy.

To counteract the adverse effects of amplitude damping in all three noisy scenarios, we introduce the escort-qubit protocol, which is discussed in detail in Sec. 3. The protocol involves introducing an auxiliary qubit, prepared in the excited state $|1\rangle$, to each resource qubit that undergoes amplitude damping during the entanglement distribution stage. A pre-noise CNOT operation is applied to entangle the resource qubit with its corresponding escort qubit, after which both qubits are transmitted through the ADC. The escort qubit effectively monitors the flip and no-flip trajectories induced by the channel. Subsequently, a second CNOT operation is applied to decouple the escort from the resource qubit, and the no-flip trajectory is post-selected, as depicted in Figs. 5, 8, and 11. This post-selection projects the shared state between the communicating parties onto a maximally entangled state, thereby restoring the superdense coding capacity to its ideal value of two classical bits.

To observe the effectiveness of our proposed escort-qubit protocol, we performed a comparative study of the superdense coding capacity under amplitude damping noise for three different noisy configurations as depicted in Fig. 14. In the absence of any protection mechanism, the superdense coding capacity decreases monotonically with increasing values of the dimensionless parameter γt, reflecting the progressive loss of entanglement and the reduced distinguishability of the encoded quantum states due to decoherence. A comparison of the three noisy scenarios reveals that the degradation of the superdense coding capacity is weakest when noise acts only on Alice's subsystem, whereas stronger suppression is observed when noise affects Bob's subsystem or both subsystems simultaneously. This behavior reflects the increasing influence of decoherence on the decoding process and on the shared entangled resource, resulting in a more pronounced loss of distinguishability of the received states.

The escort-qubit protocol proposed in this work is explicitly designed to operate on the no-flip trajectory of the ADC. This trajectory corresponds to a successful conditional realization of the channel dynamics and yields the optimal superdense coding capacity of 2 bits, as indicated by the dotted line in each panel of Fig. 14. The invariance of this capacity with respect to both the noise strength and the noisy configuration underscores the ability of the escort-qubit protocol to fully protect the information-carrying correlations when post-selection is employed.

In a realistic noisy quantum channel, however, all Kraus trajectories occur with finite probabilities. It is therefore necessary to characterize the unconditional performance of the escort-qubit protocol by introducing the average superdense coding capacity, defined as

$$\langle C_{AD}^{\mu'} \rangle = \sum_i W^i \, C_{AD}^i, \tag{41}$$

where $\mu' \in \{e_a, e_b, e_a e_b\}$ labels the escort-qubit-assisted superdense coding for the three noisy configurations disscussed in this paper, W^i denotes the probability of occurrence of the i-th Kraus trajectory of the ADC and C_{AD}^i is the corresponding superdense coding capacity associated with the output state of that trajectory. In particular, the no-flip trajectory employed in this work contributes with $C_{AD}^i = C_{AD}^{\mu'} = 2$, whereas the flip trajectories yield reduced capacities due to the degradation of entanglement. The probabilities W^i for the different ADC trajectories in the three protected noisy scenarios $\mu' \in \{e_a, e_b, e_a e_b\}$ are obtained from Eqs. 22, 29, and 36, respectively. Moreover, for the no-flip trajectory, the success probability satisfies $W^i = W^{\mu'}$ for the three cases and is given by Eqs. 24, 31, and 38.

The average capacity $\langle C_{AD}^{\mu'} \rangle$, represented by the purple solid curve in Fig. 14, quantifies the unconditional performance of the protocol in the absence of post-selection. Although the inclusion of unsuccessful trajectories inevitably results in a capacity that is suboptimal compared to the post-selected value, the average capacity consistently exceeds both the unprotected superdense coding capacity and the classical limit $C_{\rm cal} = 1$, independent of the noise configuration. This demonstrates that the escort-qubit protocol provides a genuine and robust enhancement of superdense coding performance

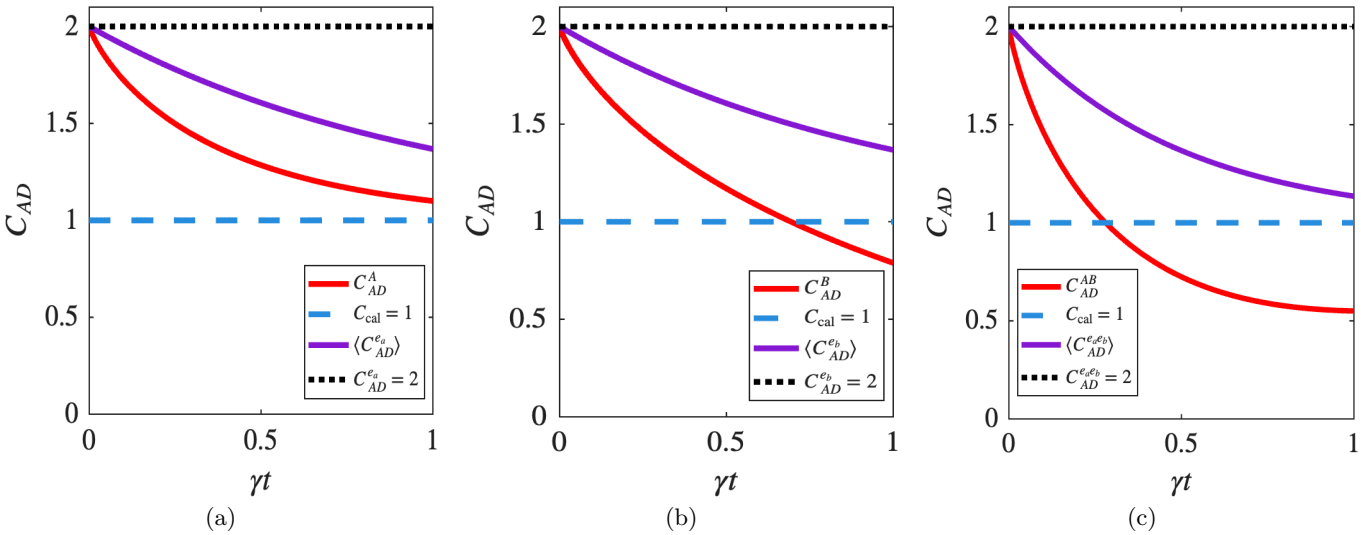


FIG. 14. Comparison of the superdense coding capacity under amplitude damping noise for three noisy configurations, with and without the escort qubit protocol. The escort qubit–assisted capacities $C^{\mu'}_{AD}$, with $\mu' \in \{e_a, e_b, e_a e_b\}$, correspond to the no-flip trajectories of the protocol when noise acts on Alice's subsystem, Bob's subsystem, and both subsystems, respectively. The corresponding average capacities, obtained by accounting for all Kraus trajectories, are also shown. Fig. 14(a) illustrates the case where only Alice's subsystem is affected by noise, Fig. 14(b) corresponds to noise acting on Bob's qubit, and Fig. 14(c) represents the general scenario in which both subsystems are subjected to noise. The dotted line denotes the escort qubit protocol capacity $C^{\mu'}_{AD} = 2$, while the purple solid line represents the average capacity $\langle C^{\mu'}_{AD} \rangle$ with $\mu' \in \{e_a, e_b, e_a e_b\}$, which remains suboptimal yet consistently above the classical limit of one bit in all cases.

even without conditioning on successful events. In conclusion, the results presented in Fig. 14 provide a clear characterization of the escort-qubit protocol by distinguishing between its conditional and unconditional performance under amplitude damping noise. While the post-selected no-flip trajectory recovers the ideal superdense coding capacity of 2 bits, the average capacity defined in Eq. (41), obtained by accounting for all Kraus trajectories of the channel, remains suboptimal. Nevertheless, this average capacity consistently exceeds that of the unprotected superdense coding scheme as well as the classical limit. Furthermore, since the superdense coding capacity associated with the no-flip trajectory is optimized to its ideal value of 2 bits independently of the noisy configuration, the escort-qubit protocol admits a natural generalization to the protection of arbitrary n-qubit entangled channels employed in quantum information protocols. In addition, the reliance of the protocol on elementary quantum operations, such as CNOT gates and projective measurements, together with the absence of complex feedback or adaptive control, suggests a comparatively favorable experimental feasibility when contrasted with other decoherence-mitigation strategies. These features make the escort-qubit protocol a practically relevant approach for enhancing superdense coding performance in realistic noisy quantum communication settings.

DECLARATIONS

Authors' contributions

JAM and MQL conceptualized,drafted and revised the manuscript. PAG is thesis supervisor of JAM. All authors approved the final manuscript.

Data availability

All relevant data are contained within the article. No new datasets were generated or analyzed during the current study.

Ethics approval

Not applicable.

Consent to participate

Not applicable.

Consent for publication

Not applicable.

Competing interests

The authors declare no competing interests.

Acknowledgements

Not applicalble

Funding

The authors received no external funding for this work.

[1] C.H. Bennett, S.J. Wiesner, Communication via one- and two-particle operators on Einstein–Podolsky–Rosen states, Phys. Rev. Lett. 69 (1992) 2881–2884. https://doi.org/10.1103/PhysRevLett.69.2881

[2] X.S. Liu, G.L. Long, D.M. Tong, F. Li, General scheme for superdense coding between multiparties, Phys. Rev. A 65 (2002) 022304. https://doi.org/10.1103/PhysRevA.65.022304

[3] A.K. Pati, P. Parashar, P. Agrawal, Probabilistic superdense coding, Phys. Rev. A 72 (2005) 012329. https://doi.org/10.1103/PhysRevA.72.012329

[4] P. Agrawal, A. Pati, Perfect teleportation and superdense coding with W states, Phys. Rev. A 74 (2006) 062320. https://doi.org/10.1103/PhysRevA.74.062320

[5] W.-X. Duan, T.-J. Wang, Control power of high-dimensional controlled dense coding, Phys. Rev. A 105 (2022) 052417. https://doi.org/10.1103/PhysRevA.105.052417

[6] A. Nayak, H. Yuen, Rigidity of superdense coding, ACM Trans. Quantum Comput. 4 (4) (2023) 1–39. https://doi.org/10.1145/3593593

[7] L. Ye, G.-C. Guo, Scheme for implementing quantum dense coding in cavity QED, Phys. Rev. A 71 (2005) 034304. https://doi.org/10.1103/PhysRevA.71.034304

[8] X.-W. Wang, Z.-H. Peng, C.-X. Jia, Y.-H. Wang, X.-J. Liu, Scheme for implementing controlled teleportation and dense coding with genuine pentaqubit entangled state in cavity QED, Opt. Commun. 282 (2009) 670–673. https://doi.org/10.1016/j.optcom.2008.10.051

[9] Y.-Y. Nie, Y.-H. Li, X.-P. Wang, M.-H. Sang, Controlled dense coding using a five-atom cluster state in cavity QED, Quantum Inf. Process. 12 (2013) 1851–1857. https://doi.org/10.1007/s11128-012-0499-z

[10] S. M. Arslan, S. Al-Kuwari, T. Abbas, Superdense coding using Bragg diffracted hyperentangled atoms, IEEE J. Sel. Areas Commun. 42 (2024) 1950–1959. https://doi.org/10.1109/JSAC.2024.3380098

[11] S. Javed, A. Tayyab, M. I. Shaukat, Super dense coding out of thermal equilibrium, Phys. Scr. 99 (2024) 075106. https://doi.org/10.1088/1402-4896/ad5145

[12] S. L. Braunstein, H. J. Kimble, Dense coding for continuous variables, Phys. Rev. A 61 (2000) 042302. https://doi.org/10.1103/PhysRevA.61.042302

[13] J. Liu, Z.-W. Mo, S.-Q. Sun, Controlled dense coding using the maximal slice states, Int. J. Theor. Phys. 55 (2016) 2182–2188. https://doi.org/10.1007/s10773-015-2857-y

[14] M. Samanta, A. Patra, R. Gupta, A. Sen De, Continuous variable dense coding under realistic non-ideal scenarios, arXiv:2407.07609 (2024). https://doi.org/10.48550/arXiv.2407.07609

[15] A. Tayyab, S. Javed, M. I. Shaukat, Superdense coding for V-shaped channel and cylindrical geometry, Phys. Scr. 98 (2023) 095109. https://doi.org/10.1088/1402-4896/aced26

[16] X. Fang, X. Zhu, M. Feng, X. Mao, F. Du, Experimental implementation of dense coding using nuclear magnetic resonance, Phys. Rev. A 61 (2000) 022307. https://doi.org/10.1103/PhysRevA.61.022307

[17] D. Wei, X. Yang, J. Luo, X. Sun, X. Zeng, M. Liu, NMR experimental implementation of three-parties quantum superdense coding, Chin. Sci. Bull. 49 (2004) 423–426. https://doi.org/10.1007/BF02900957

[18] A. Harrow, P. Hayden, D. Leung, Superdense coding of quantum states, Phys. Rev. Lett. 92 (2004) 187901. https://doi.org/10.1103/PhysRevLett.92.187901

[19] J. T. Barreiro, T.-C. Wei, P. G. Kwiat, Beating the channel capacity limit for linear photonic superdense coding, Nat. Phys. 4 (2008) 282–286. https://doi.org/10.1038/nphys919

[20] B. P. Williams, R. J. Sadlier, T. S. Humble, Superdense coding over optical fiber links with complete Bell-state measurements, Phys. Rev. Lett. 118 (2017) 050501. https://doi.org/10.1103/PhysRevLett.118.050501

[21] Y. Li, H. Zhu, W. Luo, H. Cai, M. F. Karim, X. Luo, F. Gao, X. Wu, X. Zhou, Q. Song, et al., Realizing ultrahigh capacity quantum superdense coding on quantum photonic chip, npj Quantum Inf. 11 (2025) 49. https://doi.org/10.1038/s41534-025-01007-y

[22] G. Bowen, Classical information capacity of superdense coding, Phys. Rev. A 63 (2001) 022302. https://doi.org/10.1103/PhysRevA.63.022302

[23] A. S. Holevo, Bounds for the quantity of information transmitted by a quantum communication channel, Probl. Peredachi Inf. 9 (1973) 3–11 [Engl. transl.: Problems Inform. Transmission 9 (1973) 177–183]. https://www.mathnet.ru/eng/ppi903

[24] B. Schumacher, M. D. Westmoreland, Optimal signal ensembles, Phys. Rev. A 63 (2001) 022308. https://doi.org/10.1103/PhysRevA.63.022308

[25] T. Hiroshima, Optimal dense coding with mixed state entanglement, J. Phys. A: Math. Gen. 34 (2001) 6907. https://doi.org/10.1088/0305-4470/34/35/316

[26] S. K. Sazim, I. Chakrabarty, A study of teleportation and super dense coding capacity in remote entanglement distribution, Eur. Phys. J. D 67 (2013) 174. https://doi.org/10.1140/epjd/e2013-30746-9

[27] R. Laurenza, C. Lupo, S. Lloyd, S. Pirandola, Dense coding capacity of a quantum channel, Phys.

Rev. Res. 2 (2020) 023023. https://doi.org/10.1103/PhysRevResearch.2.023023

[28] X.-M. Hu, Y. Guo, B.-H. Liu, Y.-F. Huang, C.-F. Li, G.-C. Guo, Beating the channel capacity limit for superdense coding with entangled ququarts, Sci. Adv. 4 (2018) eaat9304. https://doi.org/10.1126/sciadv.aat9304

[29] Z. Shadman, H. Kampermann, C. Macchiavello, D. Bruss, Optimal super dense coding over noisy quantum channels, New J. Phys. 12 (2010) 073042. https://doi.org/10.1088/1367-2630/12/7/073042

[30] Z. Shadman, H. Kampermann, D. Bruss, C. Macchiavello, Distributed superdense coding over noisy channels, Phys. Rev. A 85 (2012) 052306. https://doi.org/10.1103/PhysRevA.85.052306

[31] Z. Shadman, H. Kampermann, C. Macchiavello, D. Bruss, A review on super dense coding over covariant noisy channels, Quantum Meas. Quantum Metrol. 1 (2013) 1. https://doi.org/10.2478/qmetro-2013-0004

[32] B.-H. Liu, X.-M. Hu, Y.-F. Huang, C.-F. Li, G.-C. Guo, A. Karlsson, E.-M. Laine, S. Maniscalco, C. Macchiavello, J. Piilo, et al., Efficient superdense coding in the presence of non-Markovian noise, Europhys. Lett. 114 (2016) 10005. https://doi.org/10.1209/0295-5075/114/10005

[33] Z. Huang, C. Zhang, H. Situ, Performance analysis of simultaneous dense coding protocol under decoherence, Quantum Inf. Process. 16 (2017) 227. https://doi.org/10.1007/s11128-017-1677-9

[34] A. Muhuri, R. Gupta, S. Ghosh, A. Sen, Superiority in dense coding through non-Markovian stochasticity, Phys. Rev. A 109 (2024) 032616. https://doi.org/10.1103/PhysRevA.109.032616

[35] Y.-L. Li, Z. Mu, X. Xiao, Different is more: quantum switch assisted superdense coding in typical Pauli channels, Phys. Scr. 100 (2025) 125104. https://doi.org/10.1088/1402-4896/ae2218

[36] M. A. Nielsen, I. L. Chuang, *Quantum Computation and Quantum Information: 10th Anniversary Edition*, Cambridge University Press, Cambridge, USA (2011). https://doi.org/10.1017/CBO9780511976667

[37] M. Erhard, M. Krenn, A. Zeilinger, Advances in high-dimensional quantum entanglement, Nat. Rev. Phys. 2 (2020) 365–381. https://doi.org/10.1038/s42254-020-0193-5

[38] S.-T. Wu, Quenched decoherence in qubit dynamics due to strong amplitude-damping noise, Phys. Rev. A 89 (2014) 034301. https://doi.org/10.1103/PhysRevA.89.034301

[39] Y. Jeong, H. Shin, Quantum correlation in squeezed generalized amplitude damping channels with memory, Sci. Rep. 9 (2019) 4035. https://doi.org/10.1038/s41598-019-40652-0

[40] S. Dutta, D. Biswas, P. Mandayam, Noise-adapted qudit codes for amplitude-damping noise, Phys. Rev. A 111 (2025) 032438. https://doi.org/10.1103/PhysRevA.111.032438

[41] V. M. Schäfer, C. J. Ballance, K. Thirumalai, L. J. Stephenson, T. G. Ballance, A. M. Steane, D. M. Lucas, Fast quantum logic gates with trapped-ion qubits, Nature 555 (2018) 75–78. https://doi.org/10.1038/nature25737

[42] H. N. Tinkey, C. R. Clark, B. C. Sawyer, K. R. Brown, Transport-enabled entangling gate for trapped ions, Phys. Rev. Lett. 128 (2022) 050502. https://doi.org/10.1103/PhysRevLett.128.050502

[43] A. Rodriguez-Blanco, K. B. Whaley, A. Bermudez, Suppressing amplitude damping in trapped ions: Discrete weak measurements for a nonunitary probabilistic noise filter, Phys. Rev. A 107 (2023) 052409. https://doi.org/10.1103/PhysRevA.107.052409

[44] B. E. Y. Svensson, Pedagogical review of quantum measurement theory with an emphasis on weak measurements, Quanta 2 (2013) 18–49. https://doi.org/10.12743/quanta.v2i1.12

[45] M.-B. Tian, G.-F. Zhang, Improving the capacity of quantum dense coding by weak measurement and reversal measurement, Quantum Inf. Process. 17 (2018) 19. https://doi.org/10.1007/s11128-017-1786-5

[46] Y.-L. Li, D.-M. Wei, C.-J. Zu, Improving the capacity of quantum dense coding via environment-assisted measurement and quantum measurement reversal, Int. J. Theor. Phys. 58 (2019) 1–9. https://doi.org/10.1007/s10773-018-3904-2

[47] Y.-L. Li, D.-M. Wei, C.-J. Zu, X. Xiao, Enhanced superdense coding over correlated amplitude damping channel, Entropy 21 (2019) 598. https://doi.org/10.3390/e21060598

[48] S. Harraz, S. Cong, J. J. Nieto, Protected quantum teleportation through noisy channel by weak measurement and environment-assisted measurement, IEEE Commun. Lett. 26 (2021) 528–531. https://doi.org/10.1109/LCOMM.2021.3138854

[49] A.-L. Song, J. Peng, N. Maihemuti, Y. Aisan, J. Tang, Quantum communication based on decoherence suppression via weak measurement and environment-assisted measurement, Int. J. Theor. Phys. 63 (2024) 165. https://doi.org/10.1007/s10773-024-05702-y

[50] Q. Wang, Z. He, Protecting coherence by weak measurement and quantum measurement reversal, Laser Phys. 34 (2024) 105201. https://doi.org/10.1088/1555-6611/ad71b1

[51] J. A. Malik, M. Q. Lone, P. A. Ganai, Environment-assisted and weak measurement strategies for robust bidirectional quantum teleportation, Eur. Phys. J. Plus 140 (2025) 709. https://doi.org/10.1140/epjp/s13360-025-06634-0

[52] V. Abhignan, B. B. Boruah, R. Srikanth, A. Singh, Effect of weak measurement reversal on quantum correlations in a correlated amplitude damping channel, with a neural network perspective, Phys. Scr. 100 (2025) 075120. https://doi.org/10.1088/1402-4896/ade1b2